Rev. Roum. Sci. Techn.– Électrotechn. et Énerg.
Vol. **69**, *2*, pp. 147–152, Bucarest, 2024

HYBRID TYPE-1 AND 2 FUZZY SLIDING MODE CONTROL OF THE INDUCTION MOTOR

RIYADH ROUABHI, ABDELGHAFOUR HERIZI, SALIM DJERIOU, ABDERRAHIM ZEMMIT

Keywords: Analysis for comparison; Fuzzy logic; Hybrid control; Induction motor; Modelling; Sliding mode.

This paper focuses on developing two innovative induction motor (IM) control techniques. These techniques are based on the hybridization of Lyapunov theory (sliding mode) and artificial intelligence (type 1 and type 2 fuzzy logic). We will then compare these two control techniques to determine which is more robust. This comparative analysis will be based on a series of tests that we have carried out, covering the system's transient and steady-state operations under identical conditions. The first test involves observing the simulation results obtained by applying these control techniques to the motor to control the generated mechanical power. This qualitative comparison enables these controls to be evaluated for and without the application of external variations. The second test quantifies the different control laws based on quantified measurements, highlighting the performance of each technique in terms of error and time. This test is called a quantitative comparison. Finally, the last examination involves altering the machine parameters, as these values naturally experience fluctuations caused by diverse physical phenomena like inductance saturation and heating of the resistors. This comparison enables the robustness of the control techniques to be assessed.

1. INTRODUCTION

Today, the use of induction machines in industry is crucial, particularly in drive motors. This importance has prompted experts in the field to undertake in-depth research to improve the efficiency of these motors by optimizing energy transfer. This requires implementing appropriate control techniques capable of compensating for the internal and external disturbances affecting our machines. This research aims to ensure these motors operate optimally and reliably in a demanding industrial environment [1–3].

Among the various control techniques used to control our machine, sliding mode control stands out for its adaptability to systems with variable structures. The basic idea of this approach is to constrain and draw the system's dynamics (state) to a specifically chosen region, called the sliding surface, to design a control law that will constantly keep the system within this region. This way, precise and stable control can be guaranteed, even when system conditions change [4–6].

On the other hand, fuzzy logic-based control, whether type 1 or 2, is a control technique that exploits rules to deal effectively with uncertainties and non-linearities. This approach is based on the use of linguistic variables and fuzzy rules to approximate human-like decision-making processes. In this way, adaptive and robust control can be achieved, adapting to variations and changing conditions in the system. Thanks to this method, it is possible to achieve precise and reliable control, even in complex and unpredictable environments [7–9]. The combination of the strengths of sliding mode control and fuzzy logic control has attracted increasing interest in recent years, resulting in an innovative control strategy known as hybrid control. This approach seeks to exploit the advantages of both control techniques to improve performance, increase robustness, and ensure greater adaptability to induction machine systems. By synergistically combining the characteristics of the two approaches, hybrid control offers the potential to achieve superior results. It provides precise and responsive control, capable of effectively managing the uncertainties, non-linearities and variations inherent in the operation of induction motors. Thanks to this innovative control strategy, it is possible to significantly improve the performance and efficiency of industrial systems based on induction machines [10–12].

This paper presents a new hybrid control approach that combines two control techniques: sliding mode and type 1 and 2 fuzzy logic. We aim to achieve continuous and precise control of the mechanical power produced by the induction machine with almost zero tracking error and to ensure the system's robustness and stability. This innovative approach has resulted in high efficiency and optimum transmission quality.

In the first part, we presented the modeling of our machine and its bidirectional converters. In the second part, we discussed the control techniques used to control and optimise the mechanical energy generated by our machine. To this end, we have developed the following sliding mode control I based on the choice of sliding surface and convergence condition. This approach has enabled us to create a suitable control law to bring the errors between these surfaces and their controlled values toward zero. In this way, we ensure the instant stability and equilibrium of the system. II: The second control is based on hybridizing two control techniques: sliding mode and type 1 fuzzy logic. We have replaced the "signs" functions with type 1 fuzzy controllers to solve the interference problems III. The third control is also based on hybridizing two techniques: sliding mode control and type 2 fuzzy logic. This approach aims to improve the system's tracking qualities and obtain results with fewer static errors. Finally, the last part of our work is devoted to a comparative study of these control techniques. The aim is to highlight their effectiveness and robustness. This study relies on three fundamental criteria evaluated during transient and steady-state operations.

2. MODELLING OF THE MACHINE AND ITS CONVERTERS

It is necessary to model our machine and its converters individually to simulate the IM's behavior in different situations and to understand the control techniques that govern it.

2.1 IM MODEL

The induction motor is a highly complex, non-linear system. Accurate mathematical modeling is essential to effectively control its various operating modes. This

[1] Department of Electrical Engineering, Faculty of Technology/ LGE Research Laboratory, Mohamed Boudiaf University of M'sila (28000), Algeria. Emails: riyadh.rouabhi@univ-msila.dz, abdelghafour.herizi@univ-msila.dz, salim.djeriou@univ-msila.dz, abderrahim.zemmit@univ-msila.dz

DOI: 10.59277/RRST-EE.2024.69.2.5

approach provides a satisfactory and realistic representation of its behavior. The following expressions represent the mathematical model of the IM in the Park reference frame linked to the rotating field [13–17]:

$$\begin{cases} \frac{dI_{sd}}{dt} = -\frac{1}{L_s\sigma}\left(R_s + R_r\frac{M^2}{L_r^2}\right)I_{sd} + w_s I_{sq} + \cdots \\ \quad \ldots + \frac{MR_r}{L_s L_r^2\sigma}\varphi_{rd} + \frac{1}{L_s L_r\sigma}\varphi_{rq}w + \frac{1}{\sigma L_s}v_{sd} \\ \frac{dI_{sq}}{dt} = -\frac{1}{L_s\sigma}\left(R_s + R_r\frac{M^2}{L_r^2}\right)I_{sq} - w_s I_{sd} + \cdots \\ \quad \ldots + \frac{MR_r}{L_s L_r^2\sigma}\varphi_{rq} - \frac{M}{\sigma L_s}\varphi_{rd}w + \frac{1}{\sigma L_s}v_{sq} \\ \frac{d\varphi_{rd}}{dt} = \frac{MR_r}{L_r}I_{sd} - \frac{R_r}{L_r}\varphi_{rd} + w_r\varphi_{rq} \\ \frac{d\varphi_{rq}}{dt} = \frac{MR_r}{L_r}I_{sq} - \frac{R_r}{L_r}\varphi_{rq} - w_r\varphi_{rd} \\ \frac{d\Omega}{dt} = \frac{PM}{JL_r}\left(\varphi_{rd}\,I_{sq} - \varphi_{rq}\,I_{sd}\right) - \frac{C_r}{J} - \frac{f}{J}\,\Omega \end{cases} \quad 1)$$

2.2 STATOR-SIDE CONVERTER MODEL

We must use a static converter, such as an inverter, to drive our variable speed motor and supply the machine's stator. The primary aims of this converter encompass transforming the dc bus voltage into a suitable voltage for energizing the stator winding while enabling the implementation of directives to govern the mechanical power generated by the motor. The two-level converter consists of three arms, each fitted with two switches. Each switch is associated with a recovery diode mounted in antiparallel with the corresponding controllable semiconductor. The mathematical model of the stator side converter is [18–20].

$$\begin{bmatrix} V_A \\ V_B \\ V_C \end{bmatrix} = \frac{E}{6}.\begin{bmatrix} 2 & -1 & -1 \\ -1 & 2 & -1 \\ -1 & -1 & 2 \end{bmatrix}\begin{bmatrix} S_1 \\ S_2 \\ S_3 \end{bmatrix} \quad (2)$$

2.3 GRID-SIDE CONVERTER MODEL AND CONTROL

The Grid-side (GSC) offers a major advantage: it controls active power while maintaining the dc bus voltage at a constant value. In addition, it sets the reference reactive power to zero, which avoids any deterioration in the quality of the network (a unitary power factor) [21,22]:

The structure of a grid-side converter can be deconstructed into three crucial components: the energy source, the converter unit, and the connected output. The equations describing the models of these elements are as follows:

$$\frac{d}{dt}\begin{bmatrix} i_1 \\ i_2 \\ i_3 \end{bmatrix} = \begin{bmatrix} -\frac{R}{L} & 0 & 0 \\ 0 & -\frac{R}{L} & 0 \\ 0 & 0 & -\frac{R}{L} \end{bmatrix}\begin{bmatrix} i_1 \\ i_2 \\ i_3 \end{bmatrix} + \frac{1}{L}\begin{bmatrix} V_1 - V_{an} \\ V_2 - V_{bn} \\ V_3 - V_{cn} \end{bmatrix} \quad (3)$$

$$\begin{bmatrix} V_A \\ V_B \\ V_C \end{bmatrix} = \frac{Uc}{3}.\begin{bmatrix} 2 & -1 & -1 \\ -1 & 2 & -1 \\ -1 & -1 & 2 \end{bmatrix}\begin{bmatrix} S_1 \\ S_2 \\ S_3 \end{bmatrix} \quad (4)$$

$$\frac{dUc}{dt} = \frac{1}{C}\,(i_s - i_L) \quad (5)$$

The GSC control can be implemented using a cascade control structure. Two internal loops are used to control the phase currents, while an external loop is used to control the output voltage. The voltages and powers used to perform this cascade control of our grid-side converter in Park's frame of reference are expressed by [22,23]:

$$\begin{cases} V_{pd} = V_d - R\,i_d - L\frac{di_d}{dt} + L\omega i_q \\ V_{pq} = V_q - R\,i_q - L\frac{di_q}{dt} - L\omega i_d \end{cases} (6); \begin{cases} P = \frac{3}{2}.\left[V_d I_d + V_q I_q\right] \\ Q = \frac{3}{2}.\left[V_q I_d - V_d I_q\right] \end{cases} \quad (7)$$

We pose:

$$P_{ref} = U_{cmes}\,I_{red\_ref} \quad (8)$$

$$Q_{ref} = 0 \quad (9)$$

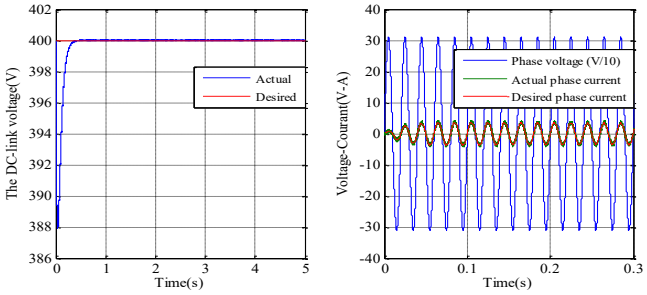

Fig. 1 – Dc bus voltage and current with line voltage.

The dc voltage has the same profile as the imposed reference voltage. In addition, the line currents faithfully reflect the characteristics of the reference currents, which have sinusoidal shapes and are in phase with the line voltage.

The results obtained successfully demonstrate the efficiency and robustness of current control in the (d,q) reference frame of the GSC. This approach results in a significant reduction in harmonics and a significant improvement in the power factor.

3. MECHANICAL POWER CONTROL

To improve the efficiency of our induction motor through better energy transfer, we need to develop suitable control algorithms that can compensate for the effects of parametric and external disturbances, thereby optimizing the control of the mechanical power produced by our machine. To achieve this, we are developing three control strategies: Sliding mode control, hybrid type-1 fuzzy sliding mode control, and Hybrid type-2 fuzzy sliding mode control.

3.1 MECHANICAL POWER BASED ON SLIDING MODE CONTROL

Sliding mode control is a recent approach to controlling non-linear systems with variable structures. This control method ensures results with fewer static errors and a fast, accurate response and is known for its stability and robustness. This control aims to control the rotational speed generated by the IM to that of a reference [24–27]. The fundamental concept of this control lies in the obligation and attraction of the dynamics (state) of the system towards a specifically defined zone, called the "sliding surface". A control law is then designed to keep the system constantly within this zone, thus guaranteeing optimal and stable control [28–30]. The model used, equations (1), is all expressed in a fixed frame of reference linked to the stator at Park reference frame (d,q).

To apply our control technique. We need to choose three sliding surfaces as follows:

The speed surface $s(\Omega) = \Omega_{ref} - \Omega$ (10)

Direct stator current surface $s(I_{sd}) = I_{sd}^{ref} - I_{sd}$ (11)

Quadrature stator current surface $s(I_{sq}) = I_{sq}^{ref} - I_{sq}$ (12)

All three sliding surfaces must be zero for the selected variables to converge to their reference values.

$$\begin{cases} s(\Omega) = \Omega_{ref} - \Omega \\ s(I_{sd}) = I_{sd}^{ref} - I_{sd} \\ s(I_{sq}) = I_{sq}^{ref} - I_{sq} \end{cases} \Rightarrow \begin{cases} \frac{d}{dt}(\Omega_{ref} - \Omega) = 0 \\ \frac{d}{dt}(I_{sd}^{ref} - I_{sd}) = 0 \\ \frac{d}{dt}(I_{sq}^{ref} - I_{sq}) = 0 \end{cases} \quad (13)$$

When the convergence conditions are satisfied, the velocity and currents tend exponentially towards their reference values, and following these values is sufficient to make the sliding surface attractive and invariant. The sliding mode is obtained provided that the Lyapunov attractivity relation is less than zero, *i.e*.,

$$s(\dot{\Omega}).s(\Omega) \leq 0 \quad (14)$$

3.1.1 SPEED CONTROL

The velocity slip surface's expression and its derivative are

$$s(\Omega) = \Omega_{ref} - \Omega \quad (15); \qquad s(\dot{\Omega}) = \dot{\Omega_{ref}} - \dot{\Omega} \quad (16)$$

$$\frac{d\Omega}{dt} = \frac{PM}{JL_r}(\varphi_{rd} I_{sq}) - \frac{C_r}{J} - \frac{f}{J}\Omega \quad (17)$$

Replacing the derivative of the velocity in equation (16) becomes

$$s(\dot{\Omega}) = \dot{\Omega_{ref}} - (\frac{PM}{JL_r}(\varphi_{rd} I_{sq}) - \frac{C_r}{J} - \frac{f}{J}\Omega) \quad (18)$$

$$s(\dot{\Omega}) = -v_1 \, sign(s(\Omega)) \quad (19)$$

$$\dot{\Omega_{ref}} - (\frac{PM}{JL_r}(\varphi_{rd} I_{sq}) - \frac{C_r}{J} - \frac{f}{J}\Omega) = -v_1 \, sign(s(\Omega)) \quad (20)$$

$$\frac{PM}{JL_r}(\varphi_{rd} I_{sq}) = v_1 \, sign(s(\Omega)) + \dot{\Omega_{ref}} + \frac{C_r}{J} + \frac{f}{J}\Omega \quad (21)$$

$$I_{sq} = \frac{JL_r}{PM\varphi_{rd}}\left(v_1 \, sign(s(\Omega)) + \dot{\Omega_{ref}} + \frac{C_r}{J} + \frac{f}{J}\Omega\right) \quad (22)$$

$$\begin{cases} I_{sqeq} = \frac{JL_r}{PM\varphi_{rd}}\left(\dot{\Omega_{ref}} + \frac{C_r}{J} + \frac{f}{J}\Omega\right) \\ I_{sqat} = \frac{JL_r}{PM\varphi_{rd}}\left(v_1 \, sign(s(\Omega))\right) \end{cases} \quad (23)$$

3.1.2 QUADRATURE STATOR CURRENT CONTROL

The expression for the quadrature current slip surface and its derivative is

$$s(I_{sq}) = I_{sq}^{ref} - I_{sq} \quad (24); \qquad s(\dot{I_{sq}}) = \dot{I_{sq}^{ref}} - \dot{I_{sq}} \quad (25)$$

$$\dot{I_{sq}} = -\frac{1}{L_s\sigma}\left(R_s + \frac{R_r M^2}{L_r^2}\right) I_{sq} - w_s I_{sd} + \frac{MR_r}{L_s L_r^2 \sigma}\varphi_{rq} - \frac{M}{L_s\sigma}\varphi_{rd} w + \frac{1}{\sigma L_s} v_{sq} \quad (26)$$

Replacing the current derivative in eq. (25) becomes:

$$s(\dot{I_{sq}}) = \dot{I_{sq}^{ref}} - (-\frac{1}{L_s\sigma}\left(R_s + \frac{R_r M^2}{L_r^2}\right) I_{sq} - w_s I_{sd} + \frac{MR_r}{L_s L_r^2 \sigma}\varphi_{rq} - \frac{M}{L_s\sigma}\varphi_{rd} w + \frac{1}{\sigma L_s} v_{sq}) \quad (27)$$

$$s(\dot{I_{sq}}) = -v_2 \, sign(s(I_{sq})) \quad (28)$$

$$\dot{I_{sq}^{ref}} + \frac{1}{L_s\sigma}\left(R_s + \frac{R_r M^2}{L_r^2}\right) I_{sq} + w_s I_{sd} - \frac{MR_r}{L_s L_r^2 \sigma}\varphi_{rq} + \frac{M}{L_s\sigma}\varphi_{rd} w - \frac{1}{\sigma L_s} v_{sq} = -v_2 \, sign(s(I_{sq})) \quad (29)$$

$$v_{sq} = \sigma L_s \dot{I_{sq}^{ref}} + \left(R_s + \frac{R_r M^2}{L_r^2}\right) I_{sq} + \sigma L_s w_s I_{sd} - \frac{MR_r}{L_r^2}\varphi_{rq} + M\varphi_{rd} w + \sigma L_s v_2 \, sign(s(I_{sq})) \quad (30)$$

$$\begin{cases} v_{sqeq} = \sigma L_s \dot{I_{sq}^{ref}} + \left(R_s + \frac{R_r M^2}{L_r^2}\right) I_{sq} + \sigma L_s w_s I_{sd} - \cdots \\ \quad \cdots - \frac{MR_r}{L_r^2}\varphi_{rq} + M\varphi_{rd} w \\ v_{sqat} = \sigma L_s v_2 \, sign(s(I_{sq})) \end{cases} \quad (31)$$

3.1.3 DIRECT STATOR CURRENT CONTROL

The expression for the direct current slip surface and its derivative is

$$s(I_{sd}) = I_{sd}^{ref} - I_{sd} \quad (32); \qquad s(\dot{I_{sd}}) = \dot{I_{sd}^{ref}} - \dot{I_{sd}} \quad (33)$$

$$\dot{I_{sd}} = -\frac{1}{L_s\sigma}\left(R_s + R_r\frac{M^2}{L_r^2}\right) I_{sd} + w_s I_{sq} + \frac{MR_r}{L_s L_r^2 \sigma}\varphi_{rd} + \frac{1}{L_s L_r \sigma}\varphi_{rq} w + \frac{1}{\sigma L_s} v_{sd} \quad (34)$$

By replacing the current derivative in eq. (33):

$$s(\dot{I_{sd}}) = \dot{I_{sd}^{ref}} - (-\frac{1}{L_s\sigma}\left(R_s + R_r\frac{M^2}{L_r^2}\right) I_{sd} + w_s I_{sq} + \frac{MR_r}{L_s L_r^2 \sigma}\varphi_{rd} + \frac{1}{L_s L_r \sigma}\varphi_{rq} w + \frac{1}{\sigma L_s} v_{sd}) \quad (35)$$

$$s(\dot{I_{sd}}) = -v_3 \, sign(s(I_{sd})) \quad (36)$$

$$\dot{I_{sd}^{ref}} + \frac{1}{L_s\sigma}\left(R_s + R_r\frac{M^2}{L_r^2}\right) I_{sd} - w_s I_{sq} - \frac{MR_r}{L_s L_r^2 \sigma}\varphi_{rd} - \frac{1}{L_s L_r \sigma}\varphi_{rq} w - \frac{1}{\sigma L_s} v_{sd} = -v_3 \, sign(s(I_{sd})) \quad (37)$$

$$v_{sd} = L_s\sigma \dot{I_{sd}^{ref}} + \left(R_s + R_r\frac{M^2}{L_r^2}\right) I_{sd} - L_s\sigma w_s I_{sq} - \frac{MR_r}{L_r^2}\varphi_{rd} - \frac{1}{L_r}\varphi_{rq} w + L_s\sigma v_3 \, sign(s(I_{sd})) \quad (38)$$

$$\begin{cases} v_{sdeq} = L_s\sigma \dot{I_{sd}^{ref}} + \left(R_s + R_r\frac{M^2}{L_r^2}\right) I_{sd} - L_s\sigma w_s I_{sq} - \cdots \\ \quad \cdots - \frac{MR_r}{L_r^2}\varphi_{rd} - \frac{1}{L_r}\varphi_{rq} w \\ v_{sdat} = L_s\sigma v_3 \, sign(s(I_{sd})) \end{cases} \quad (39)$$

Equations (31) and (39) are used to construct a sliding mode control block diagram for our induction motor.

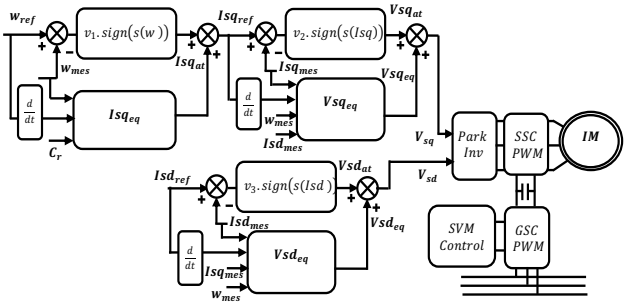

Fig. 2 – Block diagram of the sliding mode control.

3.2 MECHANICAL POWER BASED ON HYBRID TYPE-1 FUZZY SLIDING MODE CONTROL

In the field of control of electromechanical converters, research activities are increasingly directed toward the application of hybrid control technologies. This control is an attractive solution for exploiting the advantages and eliminating the disadvantages of the two control techniques combined to improve performance, increase robustness and ensure high efficiency and optimum transfer quality. In what follows, we apply the hybridization between sliding mode control and type 1 fuzzy logic to eliminate the two main drawbacks of both controls: the chattering phenomenon caused by the equivalent part of the sliding control and the instability and long computation time of the fuzzy control. This has made it possible to develop a stable and robust control system that guarantees performance results. This control system is called "hybrid type 1 fuzzy sliding control". We used the same sliding mode control structure with the three sign functions modified by type 1 fuzzy controllers to apply this control to our motor.

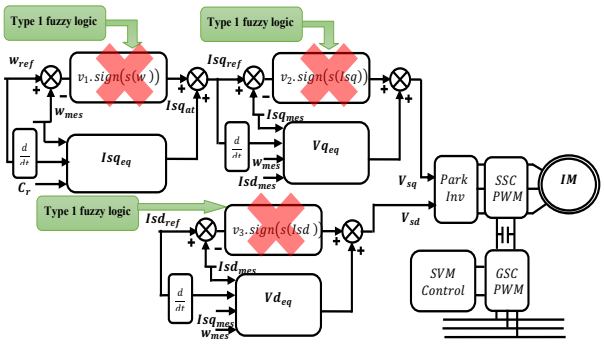

Fig. 3 – The hybrid type 1 fuzzy sliding mode control block diagram.

We used triangular shapes with trapezoidal sides to select the membership functions for the fuzzification blocks of the error and its variation. As for the choice of membership functions for the defuzzification blocks of the control variation, we also chose triangular shapes. Below is a table that presents the inference rules employed to determine the control variable related to the current parameter.

Table 1

Tabulation of the decision rules used by the type 1 fuzzy controller

The control		Error						
		NB	NM	NS	ZR	PS	PM	PB
Rate of change of error	NB	NB	NB	NB	ZR	ZR	ZR	ZR
	NB	NB	NM	NM	ZR	ZR	ZR	ZR
	NB	NB	NS	NS	PS	PS	PM	PM
	NB	NM	NS	ZR	PS	PM	PB	PB
	NM	NS	NS	PS	PS	PB	PB	PB
	ZR	ZR	ZR	PM	PM	PB	PB	PB
	ZR	ZR	ZR	PB	PB	PB	PB	PB

3.3 MECHANICAL POWER BASED ON HYBRID TYPE-2 FUZZY SLIDING MODE CONTROL

In addition to the advantages offered by hybrid type-1 fuzzy sliding control (Fig. 4), hybrid type-2 fuzzy sliding control is of particular interest because of its potential to further improve the performance achieved by its predecessor. This evolution aims to guarantee even more accurate results, significantly reducing static errors and even faster response.

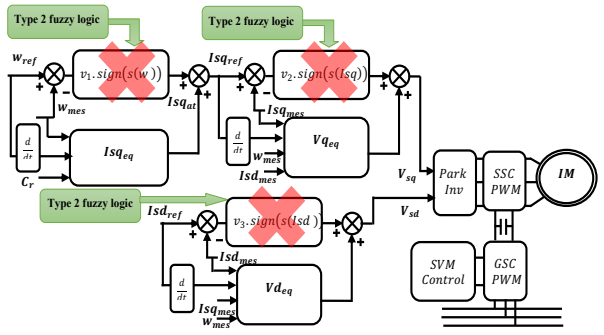

Fig. 4 – The hybrid type 2 fuzzy sliding mode control block diagram.

We systematically used the same sliding mode control structure to apply this control to our motor but replaced the three sign functions with type 2 fuzzy controllers. The differences between these three controllers lie in the values of the normalization and denormalization gains. This approach allows us to benefit from the sliding mode's advantages and take advantage of the enhanced capabilities of type 2 fuzzy controllers. These adaptations allow us to optimize the motor's performance according to our specific needs, ensuring efficient and accurate system control.

Regarding the choice of the shape of the membership functions of the fuzzification blocks of the error and its variation, we decided to use three fuzzy sets of Gaussian shapes. This choice was made because of the ability of Gaussian functions to effectively model non-linear relationships and manage uncertainties in the data. Similarly, we chose five Gaussian-shaped fuzzy sets for the control variation defuzzification block. These fuzzy sets have been carefully selected to capture different levels of control variation, allowing finer and more accurate control decisions to be made. Combining these two blocks will enable a fuzzy logic control approach that can adapt flexibly and robustly to various scenarios.

Table 2

Tabulation of the decision rules used by the type 2 fuzzy controller

The control		Error		
		N	ZR	P
Rate of change of error	N	NB	NS	PS
	ZR	NB	ZR	PB
	P	NS	PS	PB

4. COMPARATIVE ANALYSIS OF THE CONTROLS DEVELOPED

To evaluate the different control laws developed and synthesized for our engine, this paper's subject, we will conduct a comparative study of the different techniques implemented. This analysis of comparisons relies on three fundamental methodologies: qualitative, quantitative, and robust.

4.1 QUALITATIVE COMPARISONS

This comparison is based on the analysis of simulation results from the application of various control techniques developed specifically for our induction motor.

This comparison is based on the analysis of simulation results obtained by applying different control techniques developed specifically for our induction motor. In this comparison, the machine is supplied to operate at a reference speed equal to the synchronous speed of the IM (314 rad/s). An external variation is applied as a resistive torque (Cr = 2 N.m) at time T = 1s.

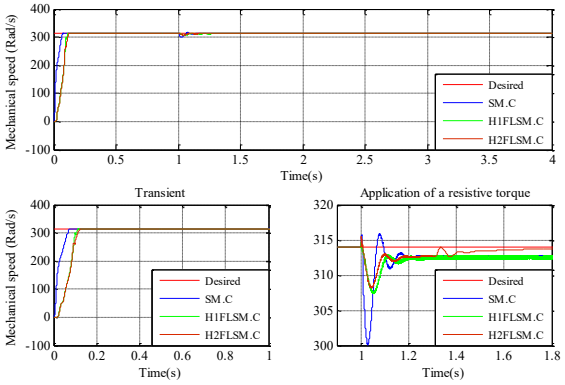

Fig. 5 –The mechanical speed produced using the three controls developed (external variation).

The simulation results show that the mechanical speed follows its reference in all three types of control. When comparing the three methods, it is necessary to compare in two stages, which are the moment of application of the resistance torque; at this stage, the sliding control (SM.C) is the worst, and this is shown by the large fluctuations compared to the other two types of control. The second stage of comparison is the response time and exponential convergence of errors; at

this stage, the results show that the control of the hybrid type 2 fuzzy sliding mode control (H.2.F.SM.C) in brown is the most responsive and closest to what is desired in red. It is followed by the hybrid type 1 fuzzy sliding mode control (H.1.F.SM.C) and, finally, by the sliding mode control.

4.2 QUANTITATIVE COMPARISONS

This assessment is based on a comparative numerical analysis of the simulation results obtained by applying the various control techniques we have developed to our induction motor. This test is based on the evaluation of four performance criteria, which are mathematically defined by Integral error squared,

$$\mathrm{ISE} = \int_0^T e^2(t)dt \quad (40)$$

The absolute error value integral: $\mathrm{IAE} = \int_0^T |e(t)|dt$ (41)

The time integral is multiplied by the absolute value of the error:

$$\mathrm{ITAE} = \int_0^T t.\,|e(t)|dt \quad (42)$$

The integral of the time multiplied by the value of the squared error: $\mathrm{ITSE} = \int_0^T t.\,e^2(t)dt$ (43)

The results shown in Table 3 are determined within the range of the external variation application (resistive torque).

Table 3

Quantitative comparison between the controls developed at the point of application of the resistive torque to the IM.

G-C	Criteria	Elaborate control systems		
		SM.C	H.1.F.SM.C	H.2.F.SM.C
Mechanical	ISE	6.4395	3.0954	1.9248
	IAE	1.1318	1.0561	0.7699
	ITAE	1.3175	1.2712	0.9065
	ITSE	6.8555	3.5210	2.1318

The simulation results in the table above clearly show that the hybrid type-2 fuzzy sliding mode control best minimizes all the ISE, IAE, ITAE, and ITSE criteria. This is reflected in the lowest values between the generated mechanical speed and its reference. This is followed by the hybrid type-1 fuzzy sliding mode control and the sliding mode control, respectively.

4.3 ROBUSTNESS COMPARISONS

The final test evaluates the developed controls' robustness by investigating how the induction motor's internal parametric variations affect their effectiveness. These parameters are subject to variations in practical scenarios due to various physical phenomena such as inductance saturation and resistance heating. In this experiment, we have varied the following parameters:

The rotor resistance Rr is multiplied by 2, and the rotor inductance Lr is divided by 2. The parameter variation is performed in the time range from $t = 1.5$ s to $t = 2.5$ s.

The matrix representation can succinctly express the standard state model for IM as:

$$[\dot{X}] = A[X] + [B][U] = ([A1] + [A2]w_s + [A3]w)[X] + [B][U] \quad (44)$$

where: $[X] = \begin{bmatrix} i_{sd} & i_{sq} & \varphi_{rd} & \varphi_{rq} \end{bmatrix}^t$; $[U] = [v_{sd} \quad v_{sq}]^T$.

$$[A] = \begin{bmatrix} -\lambda & w_s & \frac{\Gamma}{T_r} & \Gamma w \\ -w_s & -\lambda & -\Gamma w & \frac{\Gamma}{T_r} \\ \frac{M}{T_r} & 0 & \frac{1}{T_r} & (w_s - w) \\ 0 & \frac{M}{T_r} & -(w_s - w) & -\frac{1}{T_r} \end{bmatrix} = \begin{bmatrix} -\lambda & 0 & \frac{\Gamma}{T_r} & 0 \\ 0 & -\lambda & 0 & \frac{\Gamma}{T_r} \\ \frac{M}{T_r} & 0 & \frac{1}{T_r} & 0 \\ 0 & \frac{M}{T_r} & 0 & -\frac{1}{T_r} \end{bmatrix} +$$

$$+w_s \begin{bmatrix} 0 & 1 & 0 & 0 \\ -1 & 0 & 0 & 0 \\ 0 & 0 & 0 & 1 \\ 0 & 0 & -1 & 0 \end{bmatrix} + w \begin{bmatrix} 0 & 0 & 0 & \Gamma \\ 0 & 0 & -\Gamma & 0 \\ 0 & 0 & 0 & -1 \\ 0 & 0 & 1 & 0 \end{bmatrix},$$

$$[B] = \begin{bmatrix} \delta & 0 \\ 0 & \delta \\ 0 & 0 \\ 0 & 0 \end{bmatrix}; \quad \begin{cases} \lambda = \frac{1}{T_s \sigma} + \frac{1}{T_r} . \frac{1-\sigma}{\sigma} \\ \Gamma = \frac{1-\sigma}{\sigma} . \frac{1}{M} \\ \delta = \frac{1}{\sigma L_s} \end{cases} \text{ and } \begin{cases} T_s = \frac{L_s}{R_s} \\ T_r = \frac{L_r}{R_r} \end{cases}$$

To apply the robustness test, the state model is decomposed as follows:

$$[\dot{X}] = \left[\lambda[A_{11}] + \frac{\Gamma}{T_r}[A_{12}] + \frac{M}{T_r}[A_{13}] - \frac{1}{T_r}[A_{14}] + [A_2]w_s + (\Gamma[A_{31}] + [A_{32}])w\right].[X] + [B][U] \quad (45)$$

$$[A_{11}] = \begin{bmatrix} 1 & 0 & 0 & 0 \\ 0 & 1 & 0 & 0 \\ 0 & 0 & 0 & 0 \\ 0 & 0 & 0 & 0 \end{bmatrix}; [A_{12}] = \begin{bmatrix} 0 & 0 & 1 & 0 \\ 0 & 0 & 0 & 1 \\ 0 & 0 & 0 & 0 \\ 0 & 0 & 0 & 0 \end{bmatrix}$$

$$[A_{13}] = \begin{bmatrix} 0 & 0 & 0 & 0 \\ 0 & 0 & 0 & 0 \\ 1 & 0 & 0 & 0 \\ 0 & 1 & 0 & 0 \end{bmatrix}; [A_{14}] = \begin{bmatrix} 0 & 0 & 0 & 0 \\ 0 & 0 & 0 & 0 \\ 0 & 0 & 1 & 0 \\ 0 & 0 & 0 & 1 \end{bmatrix}$$

$$[A_3] = \left(\Gamma \begin{bmatrix} 0 & 0 & 0 & 1 \\ 0 & 0 & -1 & 0 \\ 0 & 0 & 0 & 0 \\ 0 & 0 & 0 & 0 \end{bmatrix} + \begin{bmatrix} 0 & 0 & 0 & 0 \\ 0 & 0 & 0 & 0 \\ 0 & 0 & 0 & -1 \\ 0 & 0 & 1 & 0 \end{bmatrix} \right)$$

As part of this comparison, we have assessed the robustness of the proposed controls by analyzing the variation in simulation results when faced with changes in machine parameters. This variation can be expressed qualitatively or quantitatively.

4.3.1 QUALITATIVE SIMULATION RESULTS

This comparison relies on examining the simulation results when confronted with parametric variations within the motor.

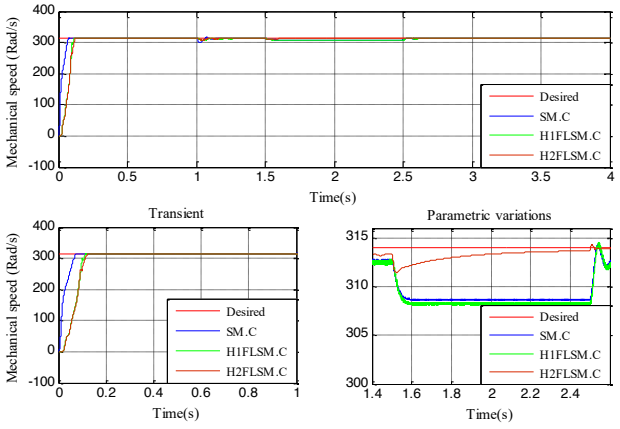

Fig. 6 – The mechanical speed produced using the three controls developed (parametric variation).

Hybrid type 2 fuzzy sliding mode control is still the best approach for achieving an almost smooth speed profile in the face of machine parametric variations.

4.3.2 QUANTITATIVE SIMULATION RESULTS

This evaluation is based on calculating the numerical differences between the simulation results at the machine's

parametric variation points. This way, ISE, IAE, ITAE, and ITSE measurements highlight each control's performance. These measurements are calculated in the time interval [1.5 s, 2.5 s].

Table 4.
Quantitative robustness comparison between the commands developed in the IM parametric variations point

G-C	Criteria	Elaborate control systems		
		SM.C	H.1.F.SM.C	H.2.F.SM.C
Mechan	ISE	27.5393	31.7864	1.0628
	IAE	5.2248	5.6102	0.8678
	ITAE	10.4993	11.2742	1.5902
	ITSE	55.4868	64.0343	1.8109

5. **CONCLUSIONS**

In this paper, we have developed two control techniques based on the hybridization of Lyapunov theory (sliding mode control) and artificial intelligence (fuzzy logic control) to regulate the mechanical power generated by our induction motor. We will then conduct a comparative study between these two approaches to determine which performs better and is more robust, both in the presence and absence of internal and external variations. The results obtained from this comparative study show that type 2 fuzzy sliding hybrid control is the best-performing and most robust for our system compared with the other control techniques used.

APPENDIX

Table 5
simulation parameters of the IM (P = 0.79 kW)

Parameters	Value	Parameters	Value
R_s	10 Ω	L_S	0.4642 H
R_r	6.3 Ω	L_r	0.4612 H
P	2	Ω	314 rad/s
f	0	J	0.02 kg. m^2

Received on 25 October 2023

REFERENCES

1. S. Lekhchine, T. Bahi, I. Abadlia, H. Bouzeria, *PV-battery energy storage system operating of asynchronous motor driven by using fuzzy sliding mode control*, International Journal of Hydrogen Energy, **42**, pp. 8756–8764 (2017).
2. A. Cavagnino, *Asynchronous Motors*, Encyclopedia of Electrical and Electronic Power Engineering, pp. 280–298 (2023).
3. J. Cheng, Y. Xiong, *Application of teaching-learning-based optimization algorithm in rotor fault diagnosis for asynchronous motor*, Procedia Computer Science, **131**, pp. 1275–1281 (2018).
4. S. Nassiri, M. Labbadi, M. Cherkaoui, *Optimal integral super-twisting sliding-mode control for high efficiency of pumping systems*, IFAC-Papers Online, **55**, *12*, pp. 234–239 (2022).
5. I. Sami, S. Ullah, *Integral super twisting sliding mode based sensorless predictive torque control of induction motor*, Power Syst., **8**, pp. 186740–186755 (2020).
6. J. Song et al., *Asynchronous sliding mode control of singularly perturbed semi-Markovian jump systems: application to an operational amplifier circuit*, Automatica, **108**, pp. 1–8 (2020).
7. M. Errouha, A. Derouich et al., *Optimization and control of water pumping PV systems using fuzzy logic controller*, Energy Rep., **5**, pp. 853–865 (2019).
8. S. El Daoudi, L. Lazrak, N. El Ouanjli, M. Ait Lafkih. *Sensorless fuzzy direct torque control of induction motor with sliding mode speed controller*, Computers & Electrical Engineering, **96**, 107490 (2021).
9. T. Ramesh, A.K. Panda, S.S. Kumar, *Type-2 fuzzy logic control-based MRAS speed estimator for speed sensorless direct torque and flux control of an induction motor drive*, ISA Transactions, **57**, pp. 262–275 (2015).
10. M.S. Adouairi, B. Bossoufi, S. Motahhir, I. Saady, *Application of fuzzy sliding mode control on a single-stage grid-connected PV system based on the voltage-oriented control strategy*, Results in Engineering, **17**, pp. 1–9 (2023).
11. R. Kavikumar et al., *Sliding mode control for IT2 fuzzy semi-Markov systems with faults and disturbances*, Applied Mathematics and Computation, **423**, *127028* (2022).
12. M. Mokhtari et al., *Sliding mode & single input fuzzy logic controllers for voltage regulation of an asynchronous wind turbine using STACOM*, IFAC Papers online, **53-2**, *22*, pp. 12803–12808 (2020).
13. D. Zellouma, Y. Bekakra, H. Benbouhenni, *Field-oriented control based on parallel proportional–integral controllers of induction motor drive*, Energy Rep., **9**, pp. 4846–4860 (2023).
14. F. Zhao et al., *The effects of parameter variations on the torque control of induction motor*, CAA International Conference on Vehicular Control and Intelligence (CVCI), Hangzhou, China (2020).
15. H. He et al., *research on active disturbance rejection control of induction motor*, IEEE 4th Advanced Information Technology, Electronic and Automation Control Conference (IAEAC 2019).
16. A. Ranjbar N, H.A. Kholerdi. *Chaotification and fuzzy PI control of three-phase induction machine using synchronization approach*, Chaos, Solitons and Fractals, **91**, pp. 443–451 (2016).
17. T. Wang, Y. Wang, Z. Zhang, Z. Li, C. Hu, F. Wang, *Comparison and analysis of predictive control of induction motor without weighting factors*, 2nd International Joint Conference on Energy and Environmental Engineering (CoEEE 22) (2022).
18. A. Benzouaoui, H. Khouidmi, B. Bessedik, *Parallel model predictive direct power control of DFIG for wind energy conversion*, Int. J. Electr. Power. Energy Syst., **125**, pp. 1–12 (2021).
19. O. Zamzoum, A. Derouich et al., *Performance analysis of a robust adaptive fuzzy logic controller for wind turbine power limitation*, Journal of Cleaner Production, **265**, pp. 1–21 (2020).
20. R. Rouabhi. R. Abdessemed. A. Chouder. A. Djerioui, *Power quality enhancement of grid-connected doubly-fed induction generator using sliding mode control*, International Review of Electrical Engineering, **10**, pp. 266–276 (2015).
21. H. Acikgoz et al., *Dc-link voltage control of three-phase PWM rectifier by using artificial bee colony-based type-2 fuzzy neural network*, Microprocessors and Microsystems, **78**, pp. 1–13 (2020).
22. J. Yang, N. Meng, *Multi-loop power control strategy of current source PWM rectifier*, Energy Rep., **8**, pp. 11675–11682 (2022).
23. L. Kou et al., *Fault diagnosis for three-phase PWM rectifier based on deep feedforward network with transient synthetic features*, ISA Transactions, **101**, pp. 399-407 (2020).
24. Y. Li, D. Wang, *Servo motor sliding mode control based on fuzzy power index method*, Computers & Electrical Engineering, **94**, 107351 (2021).
25. M.M. Lumertz, S.T.C.A. dos Santos, P.R.U. Guazzelli, C.M.R. de Oliveira, M.L. de Aguiar, J.R.B.A. Monteiro, *Performance-based design of pseudo-sliding mode speed control for electrical motor drives*, Control Engineering Practice, **132**, *105413* (2023).
26. M.M. Zirkohi, *Fast terminal sliding mode control design for position control of induction motors using adaptive quantum neural networks*, Applied Soft Computing, **115**, *108268* (2022).
27. Z. Yang, Q. Ding, X. Sun, C. Lu, H. Zhu, *Speed sensorless control of a bearingless induction motor based on sliding mode observer and phase-locked loop*, ISA Transactions, **123**, pp. 346-356 (2022).
28. Z. Yang, Q. Ding, X. Sun, H. Zhu, C. Lu, *Fractional-order sliding mode control for a bearingless induction motor based on improved load torque observer*, Journal of the Franklin Institute, **358**, pp. 3701–3725 (2021).
29. Y. Mousavi, G. Bevan, K. Beklan, A. Fekih, *Sliding mode control of wind energy conversion systems: trends and applications*, Renew Sustain. Energy Rev., **167**, pp. 1–28 (2022).
30. K. Roummani et al*., A new concept in direct-driven vertical axis wind energy conversion system under real wind speed with robust stator power control*, Renew. Energy, **143**, pp. 478-487 (2019).
31. A. Mechernene, M. Loucif, M. Zerikat, *Induction motor control based on a fuzzy sliding mode approach*, Rev. Roum. Sci. Techn.–Électrotechn. et Énerg., **64**, 1, pp. 39–44 (2019).
32. K. Makhloufi et al., *Adaptive neuro-fuzzy-slip control of a linear synchronous machine*, Rev. Roum. Sci. Techn.–Électrotechn. et Énerg. **67**, 4, pp. 425–431 (2022).